

ASTRONOMY, ASTROPHYSICS,
AND COSMOLOGY

Simulation of the Tunka-133 Scintillation Experiment

N. M. Budnev^{a,*}, A. L. Ivanova^{a,**}, N. N. Kalmykov^{b,***}, L. A. Kuz'michev^{b,****},
V. P. Sulakov^{b,*****}, and Yu. A. Fomin^{b,*****}

^a Applied Physics Institute, Irkutsk State University, bul'v. Gagarin 20, Irkutsk, 664003 Russia

^b Institute of Nuclear Physics, Moscow State University, Moscow, 119991 Russia

*e-mail: nbudnev@api.isu.ru, **e-mail: annaiv.86@mail.ru, ***e-mail: kalm@eas.sinp.msu.ru,

****e-mail: kuz@dec1.sinp.msu.ru, *****e-mail: sulakov@eas.sinp.msu.ru,

*****e-mail: fomin@eas.sinp.msu.ru

Received March 20, 2014; in final form, March 31, 2014

Abstract—The project of the scintillation complex of the upgraded Tunka-133 detector is described. Software for simulation of recording and processing of events by the future scintillation part of the Tunka-133 detector is presented. Highlights of the simulation are given. Results of the simulation of extensive air showers using Aires software are listed.

Keywords: cosmic rays, extensive air showers, EAS, Tunka-133 installation, Monte-Carlo simulation.

DOI: 10.3103/S0027134914040067

INTRODUCTION

The study of primary cosmic rays (PCRs) in the energy range of 10^{16} – 10^{18} eV is essential for the understanding their origin. At lower energies cosmic rays can be accelerated in supernova remnants in our galaxy, but in this range there should be a transition from galactic to extragalactic cosmic rays [1–5]. In this energy range the only method for studying PCRs is the detection of extensive air showers (EASs).

EAS detection in the range of 10^{16} – 10^{18} eV requires an installation with an area of ~ 1 km². The distance between the detectors should not be more than 100 m. In order to increase the amount and quality of the data about recorded EASs, it is promising to detect not one but several components of the shower by an installation, e.g., Cherenkov radiation, as well as muon and electron components [6].

The Tunka-133 installation is located in the Tunka valley in the Republic of Buryatia, 50 km from Lake Baikal. It has been used for the study of ultrahigh energy cosmic rays since 2009 [7–9]. The installation detects the Cherenkov light emitted in the atmosphere by charged particles of EASs and consists of 175 optical detectors located on an area of 3 km². Detectors are combined in 25 clusters with seven detectors in each cluster. Six detectors of a cluster are positioned at the vertices of a regular hexagon and one of the detectors is located in the center. The distance between the detectors is 85 m.

If additional scintillation detectors of muons and electrons are added to the Tunka-133 installation, in the near future it will make it possible to obtain quali-

tatively new experimental data on cosmic rays in the energy range of 10^{16} – 10^{18} eV.

1. SCINTILLATION STATIONS AT THE TUNKA-133 INSTALLATION

In 2013, the deployment of a network of scintillation stations was started that is intended for joint operation with the Tunka-133 installation.

Each scintillation station of the Tunka-133 installation [7] will include an electron detector consisting of 12 local scintillation detectors with a total area of 8 m² and a muon detector with a total area of 5 m² consisting of eight similar local detectors. The muon detector will be placed under a soil layer of 1.5 m in the immediate vicinity of the electron detector. It is planned that electron scintillation detectors will be installed in special containers at a distance of not more than 30 m from the center of the inner clusters of the Cherenkov Tunka-133 installation.

The electronics of the scintillation station largely coincide with the electronics of the cluster of the Tunka-133 installation. Two six-channel analog signal adders from the electron detector are optional. The 12 local scintillation detectors that constitute an electron detector are divided into two halves and are connected to two separate adders. The stations can send information about both the arrival of the “external” trigger signal from the nearest cluster of the Tunka-133 installation and about the arrival of the signal from the “local” trigger of the electron detector. The local trigger generation condition is the signal from a relativistic particle at the output of each adder within 100 ns.

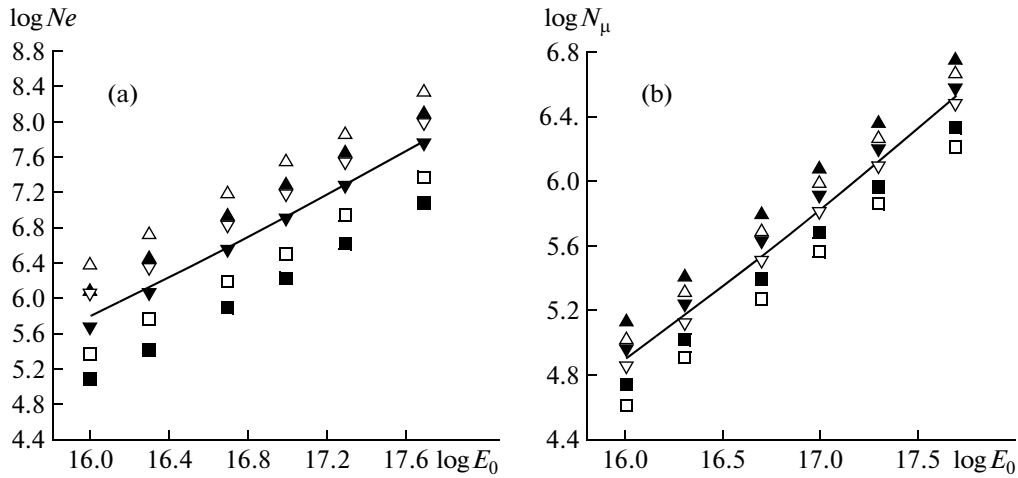


Fig. 1. The total number of electrons and the total number of muons depending on E_0 . The solid lines show approximate power functions that relate the total number of particles in the shower averaged over all angles and grades of nuclei with energies of primary particles. The points correspond to the total number of electrons (a) or muons (b) averaged over 100 showers for showers from primary protons or iron nuclei that were incident at different zenith angles \triangle — p , $\theta = 0^\circ$; ∇ — p , $\theta = 30^\circ$; \square — p , $\theta = 45^\circ$; \blacktriangle — Fe , $\theta = 0^\circ$; \blacktriangledown — Fe , $\theta = 30^\circ$; \blacksquare — Fe , $\theta = 45^\circ$.

The total scintillation complex will contain 19 scintillation stations located on the territory of the Cherenkov Tunka-133 installation in a circle with a radius of ~ 400 m. Initially the scintillation area of the installation area will be about 0.5 km^2 .

2. RESULTS OF THE CALCULATION OF ARTIFICIAL SHOWERS

The development of software for the scintillation part of the Tunka-133 Cherenkov experiment was first of all aimed at evaluation of the effectiveness of the future installation, its energy resolution, and other significant parameters. The software is based on the results of the analysis of artificial showers derived using the Aires program, which is intended for the calculation of EASs from the primary energy and up to 10^{20} eV [10]. An advantage of Aires compared with the wide-spread CORSIKA software [11] is the ease of use and speed, and a difference in the results of not more than several percentage points at the evaluation stage is not significant.

When using Aires the EAS draw was held for the values of the primary particle energy: $\log E_0 = 16, 16.3, 16.7, 17, 17.3, 17.7$ eV for the primary proton and primary iron nuclei at three zenith angles $\theta = 0^\circ, 30^\circ$ and 45° . For vertical showers additional drawing was conducted for the values $\log E_0 = 15, 15.3, 15.7, \text{ and } 18.0$. The threshold energy of muons was selected at 0.5 GeV . The calculations of hadron interactions at ultrahigh energies were carried out within QGSJET quark–gluon strings, which satisfactorily describe the modern experimental data on hadron interactions [12]. The atmospheric parameters were in compliance with those of the Tunka valley.

The analysis of the simulation data made it possible to obtain dependences of the total number of electrons $N_e(E_0)$ and the total number of muons $N_\mu(E_0)$ on the energy of primary particles assuming a pure proton and a pure iron composition of cosmic rays for different values of the zenith angle θ . In the summation over all angles assuming an equal share of protons and iron nuclei in the primary radiation these dependences take the form (see Fig. 1a, b)

$$N_e(E_0) \sim (E_0/1 \text{ PeV})^{1.14}, \quad (1)$$

$$N_\mu(E_0) \sim (E_0/1 \text{ PeV})^{0.96}, \quad (2)$$

The standard errors in determining the power values in the specified formulas do not exceed 0.005.

The magnitude of the standard deviation of the total number of electrons is accurately approximated by a function of the form

$$\sigma(N_e/\langle N_e \rangle) \sim \sigma_0(E_0/1 \text{ PeV})^{-\beta}. \quad (3)$$

For vertical showers from primary protons $\sigma_0 = 0.50$ and $\beta = 0.1$, and for showers from primary iron nuclei at $\theta = 45^\circ$ $\sigma_0 = 0.26$ and $\beta_{\max} = 0.01$.

The standard deviation of the total number of muons is almost independent of the energy and zenith angle θ ; it is sensitive only to the mass number.

The dependence of fluctuations of the total number of electrons from the energy of the primary particles was built into the software for simulation and processing of EAS events. However, at the first stage it is sufficient to take mean square deviations of the number of muons and electrons throughout the energy range from 10^{16} to 5×10^{17} eV equal to their values averaged on the energy interval.

3. SIMULATION AND PROCESSING OF “RECORDED” EAS EVENTS

The scintillation complex simulation is as follows: the energy of the primary particle is determined by a spectrum with a single break at an energy of 2×10^{15} [13, 14]. The predetermined differential energy spectrum of primary cosmic rays (PCRs) has the form $I(E_0) \sim E_0^{-(\gamma+1)}$ [14]. The parameter $\gamma = 1.5$ at $E_0 \leq 2 \times 10^{15}$ eV and $\gamma = 2$ after the break. The available experimental data show that at energies of $\sim 10^{17}$ eV the break in the partial energy spectra, which are included in the PCR, is also achieved for iron, but the spectral index of all the particles in the region of $10^{17} - 10^{18}$ eV remains about the same value as that for energies of $10^{17} - 10^{18}$ eV ($\gamma + 1 \approx 3$) and the contents of protons and iron nuclei are roughly comparable [3, 4, 15].

When simulating the direction of arrival of the primary particle, the azimuthal angle is determined evenly from 0 to 360° , and the empirical relationship $W(\theta) \sim \cos^n \theta$, where $n = 8$, is used as the zenith angle distribution θ .

The position of the shower axis in the plane of the installation is determined evenly in the square area: $-500 \dots +500$ m along the axes of X and Y . The origin is at the center of the installation.

Next, using data from preliminary calculations, the total numbers of electrons and the total number of muons in the EAS are simulated. The total number of electrons in each individual shower was determined by a lognormal distribution whose parameters were determined so that there was a compliance with the average value of N_e by formula (1) and the mean square deviation of 0.37 reflecting the fluctuations of the total number of electrons in the considered energy range [16]. The total number of muons was determined in a similar manner but with an average value of N_μ by formula (2) and the standard deviation of 0.2. At the same time, the calculated absorption ranges of the total number of electrons and muons that did not contradict the data from [17] were taken into account. The correction factor is 0.9 for electrons and 1.3 for muons. The factor shows by how many times the number of particles at a given mass composition differs from the number of particles in a purely proton composition of PCRs.

As the spatial-distribution function (SDF) of the electrons, an empirical function with parameter s depending on the distance was taken [18]

$$\rho(r) = N_e C_{\text{nom}} \left(\frac{r}{R_m} \right)^{s(r)-2} \left(1 + \frac{r}{R_m} \right)^{s(r)-4.5}, \quad (4)$$

where $R_m = 80$ m, $s(r) = s_0 + \alpha(r)$, and the dependence $\alpha(r)$ is given in [18].

The approximation of the experimental SDF of charged particles used in the software provides a better description of the fluctuations of the electron number

density with increasing distance from the shower axis in comparison with the one used previously [18].

The Greisen function is used as the muon SDF [19]. The parameters of this function are determined by the following calculations

$$\rho_\mu = N_\mu C_{\text{nom}} \left(\frac{r}{R_0} \right)^{-a} \left(1 + \frac{r}{R_0} \right)^{-b}, \quad (5)$$

where $R_0 = 180$ m and $a = 0.61$ are fixed and b varies with a mean of 2.6 and $\sigma(b) = 0.3$. The parameters s_0 and b of the electron SDF and muon SDF are associated with the age of the EAS. These parameters increase as the shower develops in the atmosphere.

Next, the densities of the electrons and muons in the EAS in detectors of the installation are found and the number of particles that enter these detectors is determined.

The number of particles, m , that are caught in each scintillator of the electron detector and in each muon detector is simulated by the Poisson law [20] with the parameter $\langle m \rangle = \rho \sigma \cos \theta$ for $(\rho \sigma) \leq 25$ or by a normal distribution [20] for $(\rho \sigma) > 25$, where ρ is the muon number density per 1 m^2 and σ is the area of the scintillator in the case of operation with an electron detector or a muon detector.

After determining the numbers of particles in each detector, time delays of particle arrivals are determined relative to the EAS plane front and the given front slope, which depends on the number of particles and measurement accuracy of the passage time of a particle through the detector. It was assumed that the time measurement accuracy was 10 ns. The delay for each meter being was determined from the Gaussian distribution with a mean value

$$\tau_{\text{geom}_{i,k}}(\text{ns}) = (\cos \varphi \sin \theta x_{i,k} + \sin \varphi \sin \theta y_{i,k} + \cos \theta z_{i,k}) / 0.3, \quad (6)$$

where $(x_{i,k}, y_{i,k}, z_{i,k})$ are coordinates of local scintillation detectors, $i = 1, \dots, 19$ is the detector number, $k = 1, \dots, 12$ is the local detector number, and the mean square deviation is 10 ns. The minimum of all delays in individual scintillators was selected as a delay that characterizes the electron detector in general.

Next, random coincidences for detectors of electrons and muons are determined taking into account the average count rate of the detector and the specified time window for the EAS detection.

The EAS event was considered “recorded” if the local trigger went off at least at three scintillation stations.

The results of the simulation were used to form output files about recorded EASs, whose parameters are then recovered using the event-processing software.

The processing program includes (1) the calculation of the main EAS parameters such as the direction of arrival, the axis position in the installation plane,

Mean errors of EAS parameter recovery formed by primary protons and iron nuclei with energies of $16 < \log E_0 < 18$

Error	Mean value	Number of events
dE_0/E_0	0.152	1338259
dN_e/N_e	0.104	1338259
dN_μ/N_μ	0.254	164980
ΔR (m)	17.12	1338259
$d\theta\varphi$ (degrees)	1.370	1338259
Δs	0.011	1338259

the total number of charged particles, and the total number of muons with an energy >0.5 GeV, (2) the reduction of the primary particle energy, (3) the comparison of source and processed distributions on E_0 , N_e , N_μ , θ , and φ , and (4) estimation of parameter measurement errors depending on the energy of the primary particle and the construction of spectra E_0 , N_e , N_μ using recovered EAS parameters and their comparison with original spectra.

At the first stage of event processing according to electron detectors the shower arrival direction is calculated under the assumption of a flat EAS front. To do this, three stations are found with the highest recorded number of charged particles and the system of three equations is solved that relates the particle arrival times in selected detectors with the direction of the EAS axis. Next, the position of the EAS axis in the plane of the installation, the total number of electrons N_e , and the total number of muons N_μ are calculated. In this case, the method of maximum likelihood is used [20]. The reduced energy value of the primary particle, E_0 , is calculated by the total number of electrons.

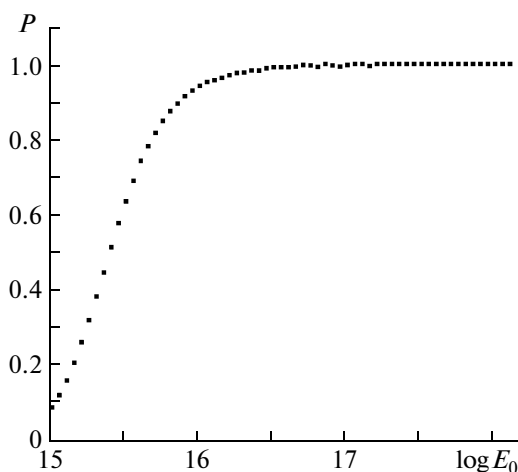


Fig. 2. The EAS detection efficiency depending on the energy of the primary particle.

In order to obtain the necessary statistics 5×10^6 recorded events were determined and processed. The table shows some of the results of this processing that make it possible to assess the average characteristics of the installation, including characteristics that indicate the quality of the simulation itself.

The effectiveness of recording events depending on the value of the energy of the primary particle that generated an EAS is shown in Fig. 2. The graph shows that the effective recording of events throughout the area of the installation (with a probability of at least 95%) starts with an energy of 10^{16} eV.

When reconstructing the energy spectrum of a PCR using the data of the new installation, a more complex energy spectrum with two break points (the second is at $E_0 = 7 \times 10^{17}$ eV) and a feature of the parabolic form in the energy range from $E_{01} = 1.2 \times 10^{17}$ eV to $E_{02} = 2 \times 10^{17}$ eV was included in the simulation software. The spectral index after the first break was $\gamma = 2$; after the second break it was $\gamma = 23$. In the simulation, the coefficients of the quadratic function are found from the boundary conditions and the requirement that the maximum amplitude of the feature should not exceed the value of the energy spectrum at $E_0 = E_{01}$ by more than 20% (see Fig. 3a,b).

The differential spectrum of a CR reconstructed by simulated events is shown in Fig. 3a, b.

Figure 3a corresponds to the energy spectrum constructed from 600000 events with the energy of the primary particle of $E_0 > 10^{16}$ eV. The number of events at $E_0 > 10^{17}$ eV is about 6000, which roughly corresponds to the statistics for a year of continuous operation of the scintillation installation. At $16 < \log E < 17$ the exponent of the initial energy spectrum $\gamma_{\text{theor}} = 2$, the exponent of the spectrum constructed by simulated events that matched the selection criterion, $\gamma_{\text{reg}} = 1.99$, and the exponent of the spectrum constructed by reconstructed events $\gamma_{\text{calc}} = 2.00$. At $17.2 < \log E < 17.7$ $\gamma_{\text{theor}} = 2$, $\gamma_{\text{reg}} = 1.97$, $\gamma_{\text{calc}} = 1.97$, after the second break $\gamma_{\text{theor}} = 2.3$, $\gamma_{\text{reg}} = 2.37$, $\gamma_{\text{calc}} = 2.38$. Standard errors in the determination of the exponent of γ for simulated and reconstructed spectra do not exceed 0.007 for the energy range of $16.0 < \log E < 17.0$, 0.03 for the interval $17.2 < \log E < 17.7$, and 0.1 for $\log E > 17.7$.

Figure 3b shows the energy spectrum constructed for 17000 events with $E_0 > 10^{17}$ eV. Such statistics roughly correspond to the expected number of events that will be recorded by a scintillation complex over 3 years of continuous operation. At $17.2 < \log E < 17.7$ $\gamma_{\text{theor}} = 2$, $\gamma_{\text{reg}} = 1.98$, $\gamma_{\text{calc}} = 1.99$, after the second break $\gamma_{\text{theor}} = 2.3$, $\gamma_{\text{reg}} = 2.37$, $\gamma_{\text{calc}} = 2.37$. The standard errors in the determination of the parameters γ_{reg} and γ_{calc} are not more than 0.007 for γ_{calc} of the energy interval $17.2 < \log E < 17.7$ and 0.04 for $\log E > 17.7$.

The reconstruction of the PCR-energy spectrum is possible using data on the EAS muon component.

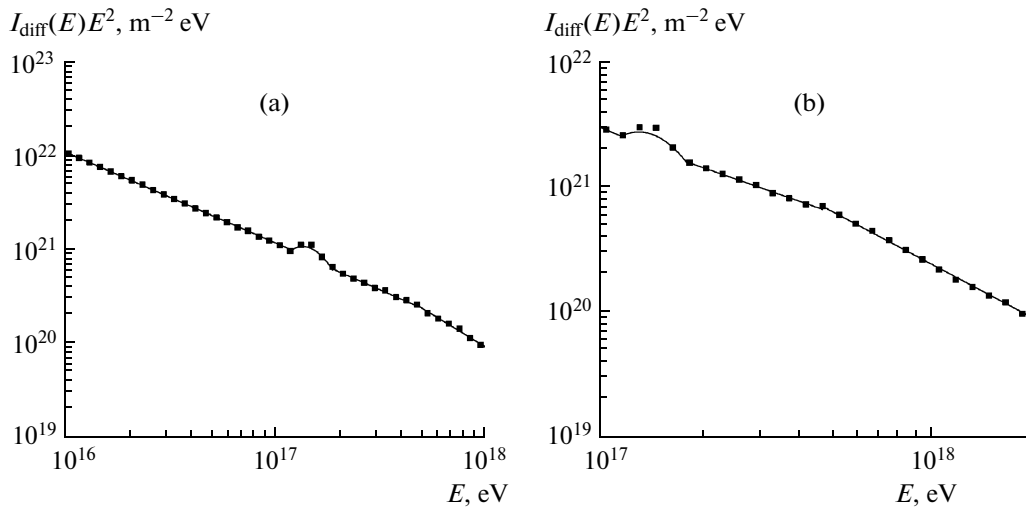


Fig. 3. The differential energy spectrum that was reconstructed using the event processing software (squares) and the spectrum constructed from simulated events for which the installation trigger condition holds true (solid lines).

However, in the adopted configuration of the future scintillation complex the chance of triggering at least three electronic detectors (the condition for triggering of the entire complex) is higher than the similar probability for muon detectors; moreover, the number of muons is reconstructed with lower accuracy (see the table). Therefore, this approach does not make much sense.

CONCLUSIONS

The existing methods for detecting real EASs are such that only fragments of information from an individual event become available to experimenters. It is possible to reconstruct the most likely parameters of the original primary particle from these fragments only by using the results of theoretical calculations.

During the analysis of the determined EASs using the Aires software the expected dependences of the total number of electrons N_e and the total number of muons N_μ on the energy of the primary particle E_0 were calculated. The results made it possible to estimate the value of the primary particle energy in each individual EAS event on the basis of data about the total number of charged particles.

The use of an SDF approximation of electrons and muons allows us to reconstruct the total number of electrons and muons in individual showers, as well as the energy spectrum of the PCR, with sufficient accuracy.

For events with energies above 10^{16} eV, the primary particle energy is reconstructed with an accuracy not worse than 15%; the total number of electrons, 10%; and the total number of muons, 25%. Such accuracy in the determination of N_μ makes it possible to analyze the mass composition of PCRs by the traditional method, i.e., by exploring distributions for a fixed N_e ,

as was done, for example, at the EAS installation at MSU [21, 22]. The absolute error in determining the position of the shower axis does not exceed 17 m at an energy of 10^{16} eV and is reduced to 5 m at an energy of 10^{17} eV.

The inclusion of scintillation detectors in the Tunka-133 installation will make it possible to record three EAS components at the same time. Therefore, it will provide researchers with qualitatively new experimental data on cosmic rays in the energy range of 10^{16} – 10^{18} eV. This and other issues related to the joint operation of the scintillation and Cherenkov parts of the installation will be discussed in our next paper.

ACKNOWLEDGMENTS

This work was supported by the Government of the Russian Federation, project no. 14.V25.31.0010, the Russian Foundation for Basic Research, project nos. 14-02-00372 and 13-02-00214, and the ISU Strategic Development Program.

REFERENCES

1. N. N. Kalmykov, P. Sulakov, Yu. A. Fomin, and J. Cotzomi, *Bull. Russ. Acad. Sci.: Phys.* **73** (5), 584 (2009).
2. S. F. Bereznev, D. Besson, A. V. Korobchenko, S. N. Epimakhov, N. I. Karpov, N. N. Kalmykov, E. E. Korosteleva, V. A. Kozhin, L. A. Kuzmichev, B. K. Lubsandorzhiev, N. B. Lubsandorzhiev, M. I. Panasyuk, E. G. Popova, V. V. Prosin, V. S. Ptuskin, B. A. Shaibonov, Jr., A. A. Silaev, A. V. Skurikhin, L. G. Sveshnikova, and I. V. Yashin, *Nucl. Inst. Meth. Phys. Res., Sec. A: Acceler., Spectrom., Detect. Assoc. Equip.* **692**, 98 (2012).
3. W. D. Apel, K. Bekk, J. Blümer, H. Bozdog, K. Daumiller, P. Doll, R. Engel, J. Engler, H. J. Gils, A. Haungs, D. Heck, T. Huege, H. O. Klages, H. J. Mathes,

- H. J. Mayer, J. Milke, J. Oehlschläger, S. Ostapchenko, T. Pierog, H. Rebel, M. Roth, A. Weindl, M. Wömmmer, J. C. Arteaga-Velázquez, F. Cossavella, D. Huber, D. Kang, K. Link, M. Ludwig, M. Melissas, N. Palmieri, M. Bertaina, E. Cantoni, A. Chiavassa, F. di Pierro, G. Navarra, I. M. Brancus, B. Mitrica, M. Petcu, G. Toma, P. Buchholz, C. Grupen, D. Kickelbrick, S. Over, P. I. Ghia, C. Morello, G. C. Trincherro, V. de Souza, D. Fuhrmann, R. Glasstetter, K. H. Kampert, J. R. Hörandel, P. Luchak, J. Zaberowski, and O. Sima, *Astropart. Phys.* **36**, 183 (2012).
4. W. D. Apel, K. Bekk, J. Blümer, H. Bozdog, K. Daumiller, P. Doll, R. Engel, J. Engler, H. J. Gils, A. Haungs, D. Heck, T. Huege, P. G. Isar, H. O. Klages, H. J. Mathes, H. J. Mayer, J. Milke, J. Oehlschläger, S. Ostapchenko, T. Pierog, H. Rebel, M. Roth, H. Schieler, F. G. Schröder, H. H. Ulric, A. Weindl, J. Wochele, J. C. Arteaga-Velázquez, M. Bertaina, E. Cantoni, A. Chiavassa, F. di Pierro, G. Navarra, F. Cossavella, M. Finger, D. Huber, D. Kang, K. Link, M. Ludwig, M. Melissas, N. Palmieri, I. M. Brancus, B. Mitrica, M. Petcu, G. Toma, P. Buchholz, C. Grupen, S. Over, P. I. Ghia, C. Morello, G. C. Trincherro, V. de Souza, D. Fuhrmann, R. Glasstetter, K. H. Kampert, J. R. Hörandel, P. Luchak, J. Zaberowski, and O. Sima, *Phys. Rev. Lett.* **107**, 171104 (2011).
 5. L. G. Sveshnikova, E. E. Korosteleva, L. A. Kuzmichev, V. S. Ptuskin, V. A. Prosin, and O. N. Strelnikova, *J. Phys.: Conf. Ser.* **409** (1), 012062 (2013). <http://iopscience.iop.org/1742-6596/409/1/012062>
 6. V. B. Atrashkevich, N. N. Kalmykov, and G. B. Khristiansen, *JETP Lett.* **33**, 225 (1981).
 7. S. F. Berezhnev, D. Besson, N. Budnev, et al., *Proc. 33rd Int. Cosmic Ray Conf.*, Rio de Janeiro, 2013.
 8. S. F. Berezhnev, S. N. Epimakhov, N. I. Karpov, N. N. Kalmykov, E. E. Korosteleva, V. A. Kozhin, L. A. Kuzmichev, M. I. Panasyuk, E. G. Popova, V. V. Prosin, A. A. Silaev, A. V. Skurikhin, L. G. Sveshnikova, I. V. Yashin, N. M. Budnev, O. A. Chvalaev, O. A. Gress, A. N. Dyachok, E. N. Konstantinov, A. V. Korobchenko, R. R. Mirgazov, L. V. Pankov, Y. A. Semenev, A. V. Zagorodnikov, B. K. Lubsandorzhev, N. B. Lubsandorzhev, B. A. Shaibonov, V. S. Ptushkin, A. Chiavassa, C. Spiering, R. Wischnewski, D. Besson, J. Snyder, M. Stockham, A. Haungs, and F. G. Schröder, *Nucl. Instr. Meth. Phys. Res., Sec. A* **692**, 98 (2012).
 9. N. M. Budnev, O. A. Gress, L. V. Pan'kov, Yu. A. Semenev, R. Wischnewski, Ch. Spiering, N. N. Kalmykov, E. E. Korosteleva, L. A. Kuzmichev, M. I. Panasyuk, Yu. V. Parfenov, V. V. Prosin, D. V. Chernov, A. V. Shirokov, I. V. Yashin, B. K. Lubsandorzhev, P. G. Pokhil, G. Navarra, and V. S. Ptuskin, *Bull. Russ. Acad. Sci.: Phys.* **73**, 395 (2005).
 10. <http://www.fisica.inpl.edu.ar/auger/aires/doc/Users-Manual.pdf>
 11. http://www-ik.fzk.de/corsika/usersguide/corsika_tech.html
 12. N. N. Kalmykov, S. S. Ostapchenko, and A. I. Pavlov, *Nucl. Phys. B* **52**, 17 (1997).
 13. G. V. Kulikov and G. B. Khristiansen, *Zh. Eksp. Teor. Fiz.* **35** (4), 635 (1958).
 14. Yu. A. Fomin, N. N. Kalmykov, G. B. Khristiansen, et al., *Proc. 16th Eur. Cosmic Ray Symp.*, Madrid, 1998, p. 261.
 15. S. F. Berezhnev, D. Besson, N. M. Budnev, et al., *Proc. 32 ICRC*, Beijing, 2011, vol. 7, p. 208.
 16. N. N. Kalmykov, *Yad. Fiz.* **10** (1), 121 (1969).
 17. M. Yu. Zotov, N. N. Kalmykov, G. V. Kulikov, and V. P. Sulakov, *Mos. Univ. Phys. Bull.* **64**, 632 (2009).
 18. N. Kalmykov, G. Kulikov, V. Sulakov, and Yu. Fomin, *Bull. Russ. Acad. Sci.: Ser. Phys.* **77**, 626 (2013).
 19. K. Greisen, in *Progress in Cosmic Ray Physics*, Ed. by J. Wilson, (Amsterdam: North-Holland, 1956; Moscow: InLit, 1958).
 20. S. M. Ermakov and G. A. Mikhailov, *Course of Statistical Simulation* (Moscow, 1976) [in Russian].
 21. Yu. A. Fomin, N. N. Kalmykov, G. B. Khristiansen, G. V. Kulikov, V. I. Nazarov, S. S. Ostapchenko, A. I. Pavlov, V. I. Solovjeva, V. P. Sulakov, A. V. Trubitsyn, and E. A. Vishnevskaya, *J. Phys. G: Nucl. Part. Phys.* **22**, 1839 (1996).
 22. N. N. Kalmykov, L. A. Kuz'michev, G. V. Kulikov, V. V. Prosin, V. P. Sulakov, and Yu. A. Fomin, *Mos. Univ. Phys. Bull.* **65**, 275 (2010).

Translated by O. Pismenov